Presented at the Institute of Navigation GPS/GNSS Conference, September 9-12, 2003, Portland, OR

Light Detection and Ranging-Based Terrain Navigation – A Concept Exploration

Jacob Campbell, Maarten Uijt de Haag, Frank van Graas, *Ohio University, Athens, Ohio*
Steve Young, *NASA Langley Research Center, Hampton, Virginia*

BIOGRAPHY

Jacob Campbell completed his B.S.E.E. at Ohio University in 1999 with concentration in the area of digital systems and computer architecture, and he completed his M.S.E.E. at Ohio University in 2001 with concentration in the area of avionics navigation systems. He received the Ohio Space Grant Consortium fellowship to conduct research in the area of Synthetic Vision of Terrain, and he is currently working on his Ph.D. at Ohio University with research in the area of airborne LiDAR systems.

Maarten Uijt de Haag is an Assistant Professor of Electrical Engineering at Ohio University and a Principal Investigator with the Ohio University Avionics Engineering Center. He earned his Ph.D. from Ohio University and holds a B.S.E.E. and M.S.E.E. from Delft University of Technology, located in the Netherlands. He has been involved with GPS landing systems' research, advanced signal processing techniques for GPS receivers, GPS/INS integrated systems, and terrain-referenced navigation systems. The latter includes the development of terrain data base integrity monitors as an enabling technology for Synthetic Vision Systems and autonomous aircraft operations.

Steve Young is a Principal Investigator for flight-critical systems research focused on civil aviation platforms; the goal of his research is to develop new avionics technologies and/or apply existing technologies to improve operational safety and efficiency. Specific research on CNS systems includes applications of data link, INS, and GPS, to safety problems such as runway incursions and controlled flight into terrain. Currently investigating integrity, reliability, and performance issues associated with proposed on-board display systems known as Synthetic Vision Systems (SVS). Steve received his BSEE from the West Virginia Institute of Technology in 1987 and his MSEE from the Georgia Institute of Technology in 1990. Steve serves as co-chair of RTCA/EUROCAE Special Committee (SC-193), Sub-group 3

Frank van Graas holds a Fritz J. and Dolores H. Russ Professorship in Electrical Engineering and he is a Principal Investigator with the Avionics Engineering Center at Ohio University. He has authored or co-authored approximately 60 navigation-related publications, including two book chapters. He received RTCA's *William E. Jackson* Award for his work on integrated GPS/Loran, the *Johannes Kepler* Award for sustained and significant contributions to satellite navigation from the Satellite Division of the ION, and the *Thurlow* Award for outstanding contribution to the science of navigation from the ION. He is a Fellow of the ION and an Ohio University Presidential Research Scholar. He has been involved with navigation research and flight-testing since 1984. Most recently, he has worked on Fault Detection, GPS attitude determination, GPS/INS integrated systems, GPS landing systems, and terrain-referenced navigation systems.

ABSTRACT

This paper discusses the use of Airborne Light Detection And Ranging (LiDAR) equipment for terrain navigation. Airborne LiDAR is a relatively new technology used primarily by the geo-spatial mapping community to produce highly accurate and dense terrain elevation maps. In this paper, the term LiDAR refers to a scanning laser ranger rigidly mounted to an aircraft, as opposed to an integrated sensor system that consists of a scanning laser ranger integrated with Global Positioning System (GPS) and Inertial Measurement Unit (IMU) data. Data from the laser range scanner and IMU will be integrated with a terrain database to estimate the aircraft position and data from the laser range scanner will be integrated with GPS to estimate the aircraft attitude.

LiDAR data was collected using NASA Dryden's DC-8 flying laboratory in Reno, NV and was used to test the proposed terrain navigation system. The results of LiDAR-based terrain navigation shown in this paper indicate that airborne LiDAR is a viable technology enabler for fully autonomous aircraft navigation. The navigation performance is highly dependent on the quality of the terrain databases used for positioning and therefore

high-resolution (2 m post-spacing) data was used as the terrain reference.

1. INTRODUCTION

In general, navigation systems can be divided into two major categories; positioning systems and dead reckoning systems [1]. This paper explores a positioning system, which estimates the aircraft position using the integration of airborne laser range scanner (or LiDAR) data with a terrain elevation database. An airborne mapping LiDAR consists of a laser range scanner, an Inertial Measurement Unit (IMU), a Global Positioning System (GPS) receiver, and a data collection system. Airborne mapping LiDAR is most commonly used by the mapping community because of its capability to produce dense earth referenced terrain point clouds. Accuracies of the terrain posts (earth referenced point of terrain) are typically less than 30 cm RMS. This error is driven by the error in the kinematic GPS solution and the error in the LiDAR attitude estimation [2] [3] [4].

Terrain navigation has been around since WWII when navigators used the range and intensity returns from ground mapping radars to visually compare the location of various landmarks displayed on the radar screen with a map [1]. Other examples of terrain navigation systems developed since WWII include Terrain Contour Matching (TERCOM) and the Sandia Inertial Terrain–Aided Navigation (SITAN). TERCOM is described in [5], [6], and [7] as a method of terrain navigation in which the vehicle's position is derived by correlating a sensed terrain profile to a map terrain profile. The resulting position is input to a Kalman filter, which updates the vehicle's Inertial Navigation System (INS). In SITAN [7], [8] the INS is aided using terrain slope information as an input to a Kalman filter instead of terrain profile correlation. In [9] a combination of both TERCOM and SITAN is used to obtain a best position fix. [10] describes parallel SITAN, a bank of extended Kalman filters that process identical altimeter measurements but are centered at different latitudes and longitudes within a circular error region around the true position. The Kalman filters that diverge over time are discarded and hence the error region is reduced. In [11] the log-likelihood function of the discrepancy between changes along the sensed and map terrain profiles is investigated. The likelihood function is characterized for terrain data and approximated by a normal distribution for the use of the terrain profile change difference as an input to a Kalman filter used for terrain navigation. In [12] a correlation scheme, operating in the frequency domain, is used to provide updates to a dead reckoning system. In principle, time domain or frequency domain processing are equivalent in terms of performance, however, frequency domain processing often allows for reduced computational complexity and increased observability. Various other U.S. patents such as [13] and [14] illustrate the concept of navigation and guidance using the comparison between altimeter information and stored terrain data.

Airborne LiDAR–based terrain navigation can be used for various aircraft applications, such as en-route position and attitude determination, general positioning capabilities, runway incursion detection and obstacle detection. Depending on the required performance for each of these applications, LiDAR may have to be integrated with other sensors. For en-route position and attitude determination, integration of LiDAR with an Inertial Navigation System (INS) is envisioned whereas for a general positioning capability LiDAR plus a terrain elevation database may be sufficient. For both runway incursion and obstacle detection a LiDAR by itself may suffice.

This paper first discusses the challenges that lay ahead when LiDAR-based terrain navigation is considered for fully autonomous aircraft navigation. Next, the LiDAR system is described and the eye-safety aspects of the system are discussed. Finally, the LiDAR-based terrain navigation algorithm is presented and flight test results are described.

2. CHALLENGES

Various challenges must be overcome before LiDAR-based terrain navigation will become a technology mature enough to enable fully autonomous aircraft navigation. The first challenge is the operation of the laser range scanner under various weather conditions, such as fog, rain, cloud cover, and snow. Possible solutions are an increase in laser-transmitted power or a limit on the operational range. While these solutions are practical, they can directly affect the safety aspects of laser operation as discussed in the next paragraph. Better solutions may be the use of multi-spectral systems, improved laser detection schemes, and processing data with the aid of an IMU to allow for data correlation.

The second challenge is laser safety during LiDAR-based procedures. The main issues with regard to laser safety are first eye safety, then as power is increased, burn and fire hazards. These effects may be mitigated or reduced by a proper choice of laser frequencies to so-called eye-safe frequencies, and power limitations. The next section will discuss the eye-safety aspects in more detail.

To enable terrain-based navigation at high performance levels, reliable terrain elevation databases must be available which are both accurate and have a spatial

resolution comparable to the point spread from the LiDAR system. Availability of the databases is driven by areas of operation and may require generation of these databases through mapping missions. These missions will require both funds and time. The cost and time can be shared among all users of accurate maps and the mapping community if the necessary specifications of point density, accuracy, and integrity of these terrain databases can be shared.

The current airborne LiDAR-based mapping equipment requires both a set of aircraft procedures and post-flight processes to calibrate the laser range scanners. Such procedures are undesirable for autonomous aircraft navigation due to the time and cost to perform. Proper installation procedures and an automated calibration process should help mitigate this issue.

The final challenge is to determine the methods required to process the large amounts of laser scanner range data and the integration of this data with the terrain elevation databases in real-time. The solution to this will be found in better and more optimized algorithm design and development and design of more efficient hardware implementations.

3. EYE SAFETY CONSIDERATIONS

Given the laser power that would be needed to achieve all-weather laser ranging performance and the widespread use of near-infrared lasers, the issue of eye safety must be addressed. Many laser ranging systems in existence today use high Pulse Repetition Frequencies (PRFs) (10 – 75+ kHz) and require high power levels. One of the commonly used lasers that is able to meet these requirements is the diode pumped near-infrared 1.064 μm Nd:YAG laser. The performance and cost of the Nd:YAG laser meets the requirements of most airborne LiDAR systems, however, the eye's retina is sensitive to this wavelength and can be damaged if precautions are not taken. Thus, it may be necessary to look towards other laser technologies, which may provide high power, but operate at eye-safe frequencies.

The eye is made up of several membrane and fluid layers. Lasers which transmit in the visible, 300-400 nm to 760-780 nm wavelength, and near-infrared, 760-780 nm to 1400 nm, can cause damage to the retina of the eye due to the ability of the laser energy to travel through the cornea, the aqueous, the lens, and the vitreous humor and reach the sensitive retina [15]. Laser wavelengths longer than 1400 nm begin to be absorbed by the much less sensitive cornea and aqueous fluid, making lasers, which operate above the 1400 nm wavelength safer for the eye.

The decrease in sensitivity to wavelengths longer than 1400 nm is clearly indicated in the American National Standards Institute (ANSI) publication [16]. In the ANSI standards, a laser operating at 1064 nm with a pulse length of 10 ns (a typical Nd:YAG laser ranger specification) has a safe Maximum Permissible Exposure (MPE) value of 5×10^{-6} J/cm^2 for an exposure duration of 10^{-9} to 50×10^{-6} seconds. Given the specifications of the LiDAR used on the Reno, NV DC-8 missions, the Nominal Ocular Hazard Distance (NOHD) for an MPE of 5×10^{-6} is 426 m as computed as specified in [16]. The MPE for the same pulse length, but at a frequency of 1500 nm is 1.0 J/cm^2 which is a 200,000 times increase over the MPE of a 1064 nm wavelength laser. Applying an MPE of 1.0 J/cm^2 to the NOHD calculations leads to a NOHD of only 1 m. This illustrates the gains in safety and power, which can be achieved by the development of lasers, which operate at 1400 nm and longer wavelengths.

The development of a practical pulsed laser in the 1500 nm range has been of great interest for many years due to the significant reduction of the necessary NOHD. Current techniques to produce a 1500 nm wavelength laser feed a signal of wavelength 1000 nm to 1100 nm into an Optical Parametric Oscillators (OPO). The OPO splits the beam into an idler beam and a signal beam, the signal beam having a wavelength between 1500 nm to 2200 nm [17]. This technology has been refined by the selection of different crystals for the OPO, and has demonstrated the ability to produce a 1534.7 nm wavelength with a sustained average output signal power of 33 Watts [18], which is a power of 10 times higher than many of the lasers currently used for Airborne LiDAR Mapping.

4. LIDAR TERRAIN NAVIGATION

The LiDAR-based terrain navigation method that is considered in this paper uses the raw measurements from the LiDAR's scanning laser ranger and combines these measurements with the estimated attitude, estimated position, and a high resolution (2-m post-spacing) terrain database information to solve for position, velocity and attitude. Each LiDAR laser measurement record consists of a quadruple of data: a time-tag, t_n, a scan angle, α_n, a range, r_n, and an intensity value, I_n. Within the context of this paper the intensity values will not be used in the terrain navigation calculations.

The proposed algorithm uses all N return pulses from one back-and-forth laser scan; at a PRF of 33,333Hz and a scan rate of 20 Hz one back-and–forth scan consists of about 3,333 transmitted pulses. The result of this method is a position estimate every 0.1 seconds. At a speed of about 200 kts the aircraft moves approximately 10 m per scan as illustrated in Figure 1.

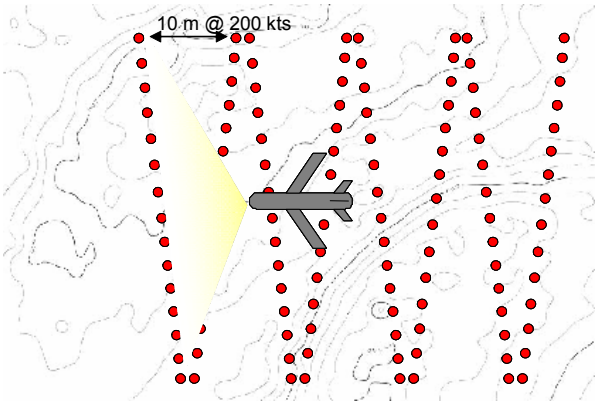

Figure 1, LiDAR Scanning Pattern

At each measurement time, t_n, the aircraft's lateral position (East-North), $\hat{x}^-(t_n)$, can be estimated from the previous position and velocity estimates. Then, all N position estimates form the track of the aircraft during one back-and-forth laser scan. These position estimates, the scan angles, and attitude information is then used to determine the range estimates to the terrain. The range estimates are obtained from the terrain elevation databases using ray-tracing. The estimated range for each t_n is given by $r_{db}(t_n)$.

The laser range estimates, $r_{db}(t_n)$, are compared to the range measurements $r_{laser}(t_n)$ from the laser range scanner by forming the Mean Square Difference (MSD) consistency metric:

$$MSD_N = \frac{1}{N}\sum_{n=0}^{N-1}\left[r_{db}(t_n) - r_{laser}(t_n)\right]^2 \qquad (1)$$

To determine if there is a residual error between the actual and estimated track the MSD is re-evaluated for a set of tracks offset from the original estimate:

$$\hat{\mathbf{x}}(k,l,t_n) = \hat{\mathbf{x}}^-(t_n) + \Delta\mathbf{x}(k,l) \qquad (2)$$

where

$$\Delta\mathbf{x}(k,l) = \left[(k\cdot\delta x) \quad (l\cdot\delta y)\right]^T \qquad (3)$$

is the track offset and $k,l = -M,\ldots,M$. δx and δy are the spatial resolution in the East and North direction, respectively, and M determines the search area.

The offset for which the MSD is minimum will be an estimate for the position residual error. Figure 2 shows a flow diagram of proposed algorithm.

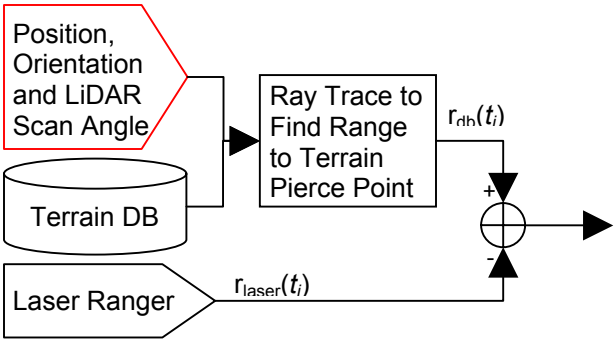

Figure 2, Flow Diagram of the Disparity Calculation

This process can be repeated for the estimation of the altitude, velocity, and attitude. Also, this method may be implemented to varying degrees; one method that would not affect the autonomy of the system is the integration of the LiDAR measurements with IMU measurements to improve the velocity and attitude estimation. Since it is expected that the position solutions developed by searching for the offset, which has the minimum MSD should not drift over time, it would provide complementary information to the IMU data. Estimation techniques such as Kalman filters could then be applied to exploit this complementary character of the data. Estimation techniques such as the Kalman filter have been used for other terrain navigation systems developed in the past, however the accuracies and amounts of uncorrelated data available make this system unique. Estimations of the LiDAR horizontal radial position accuracy seen in the results section are better than 2 m RMS for one-second of LiDAR data.

5. DC-8 FLIGHT TEST SETUP

Flight tests were conducted on July 28th, July 30th, August 1st, and August 4th with NASA's DC-8. A data collection system installed on this aircraft was used to collect LiDAR data (kinematic GPS data, IMU attitude and delta velocities, laser range scanner angle, laser range scanner range data), radar altimeter data, and weather radar data. The primary purpose of the flight test was to collect weather radar and radar altimeter data for the NASA Langley Research Center (NASA LaRC) real-time synthetic vision terrain elevation database integrity monitor. The LiDAR system installed on the DC-8 was an Optech ATLM on loan from the US Army. The goal of the data collection effort was twofold; for radar altimeter and weather radar sensor characterization; and to investigate the concept of LiDAR terrain navigation. The ALTM laser unit was mounted in the cargo bay of NASA Dryden's DC-8 Flying Laboratory which can be seen in Figure 3.

Figure 3, NASA Dryden DC-8 Flying Laboratory, Picture Retrieved from NASA Webpage.

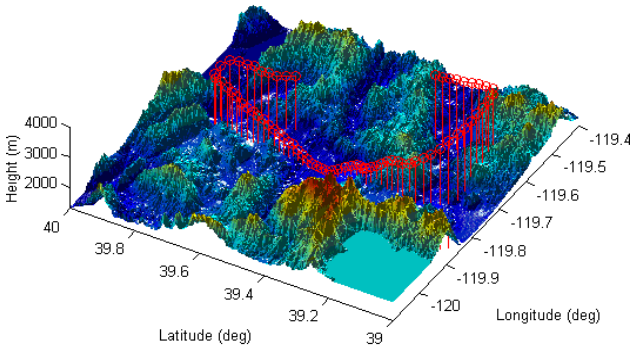

Figure 4, Flight Path of and Approach into KRNO

LiDAR data sets were collected for approaches flown into the Reno, Nevada airport (KRNO) and the aircraft was high enough above ground level for the ALTM sensor to be eye safe. An example of one of these approaches is shown in Figure 4.

Figure 5 provides a block diagram of the data collection system used on the DC-8 DIME experiment.

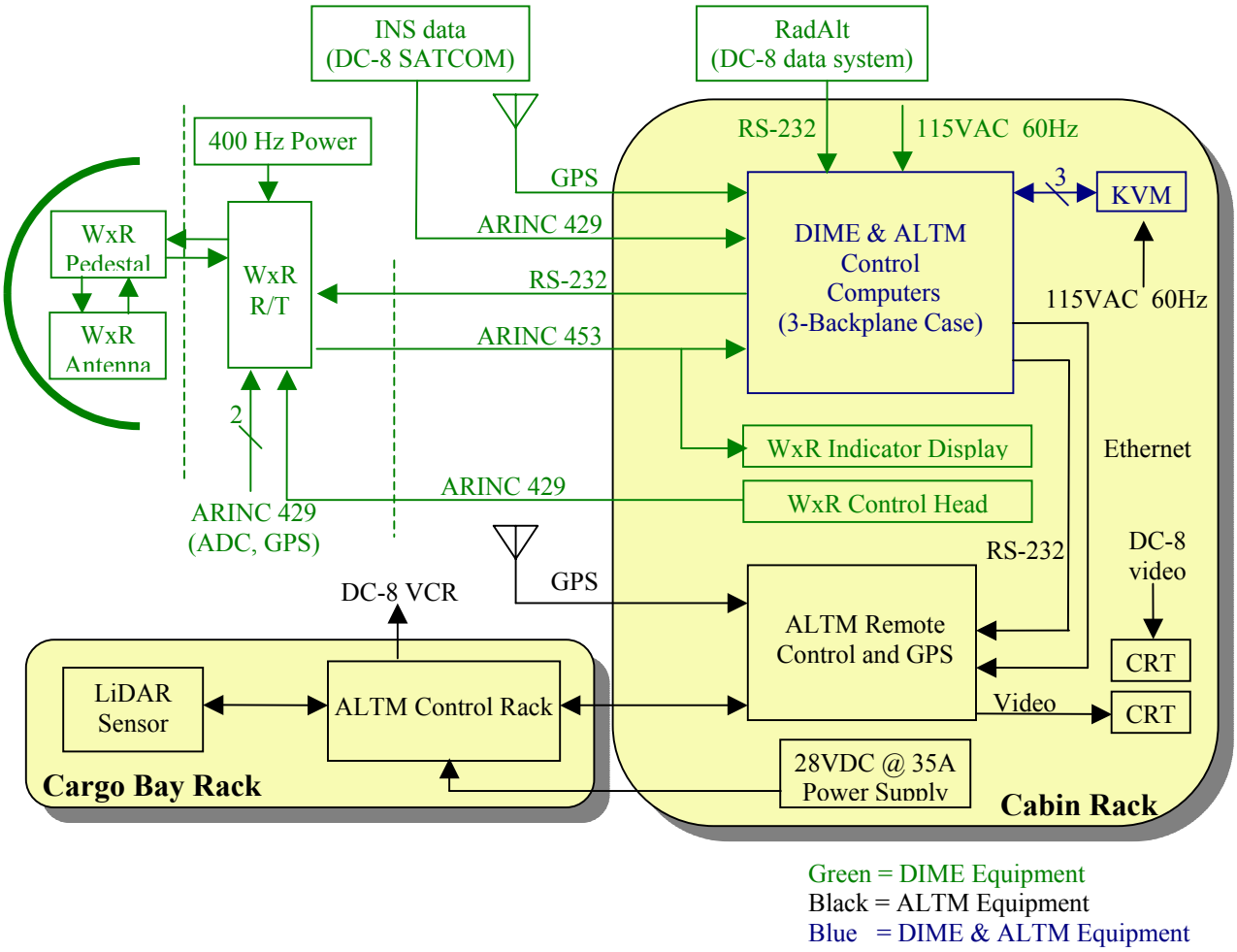

Figure 5, DC-8 DEM Integrity Monitor Equipment (DIME) & ALTM System Diagram

6. MEASUREMENT CHARATERISTICS

ALTM data sets collected on the July-August DC-8 flight tests were post-processed with the NGS, 2 m post-spacing, terrain database to solve for the aircraft's position and attitude. This section of the paper provides an analysis of the expected position and attitude accuracies when using LiDAR measurements as discussed in section 3. Results from these computations are given in the next section.

The complete Optech ALTM system uses laser range, laser scan angle, laser origin earth referenced attitude, and laser origin earth referenced position to solve for the earth referenced position of the point illuminated by the laser ranger. The approach taken in this paper to solve for the aircraft position and attitude differs from the method used for position and attitude estimation for LiDAR mapping missions.

A measurement disparity metric, $p_{disparity}(t_i)$, for time t_i was developed to assess the agreement between the range measured by the laser ranger, $r_{laser}(t_i)$, and the expected range from the aircraft to the laser pierce point in the terrain elevation database. This pierce point is computed using the true aircraft position, attitude, and scan angle in combination with a ray-tracing algorithm. The range computed from that database is referred to as $r_{db}(t_i)$. Figure 2 provides a diagram of the $p_{disparity}(t_i)$ calculation.

The sum of squares (SS) of a time sequential series of disparities is then calculated to create a measurement agreement metric t as given by (4).

$$t = \sum_{i=1}^{N} p_{disparity}(t_i)^2 \qquad (4)$$

The position and attitude measurement is found by finding the minimum t value in a search space. The search space is formed by adding constant offsets to the position or attitude (adding constant offsets to the values shown in the red box in Figure 2) over the N disparities used to form the t measurement of agreement. Thus the center or zero offset of the search space is the position or attitude measured from the kinematic GPS (< 0.20 m accuracy) or post-processed GPS aided IMU (~0.008 deg accuracy).

7. MEASUREMENT CHARACTERISTICS RESULTS

One second of data from the approach shown in Figure 4 was examined to provide some insight into the performance of the position and attitude measurements found by searching for the minimum SS as described in the previous section. Given the amounts of data to be processed and search spaces selected, the data were down-sampled by a factor of 10 (leaving 333 points per scan) making processing possible given the computing resources available (Pentium 4, 1.8 GHz with 1.2 GB of memory).

The horizontal position measurement is shown in Figures 6, 7, 8, 9, 10, and 11. The two-dimensional horizontal position search space is shown for every other 0.1 second time epoch. The center of each figure is the truth position as determined by kinematic GPS in post-processing mode. The white '∗' represents the minimum SS and thus the position estimate of the LiDAR-based terrain navigation system. The RMS value of the measured distance to the truth of this small sample of measurements is 1.7 m.

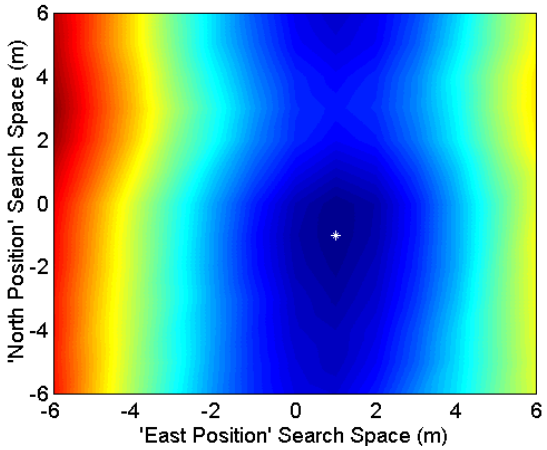

Figure 6, Position Search at GPS Time = 315280.0883 '∗' Marks Minimum Sum of Squares

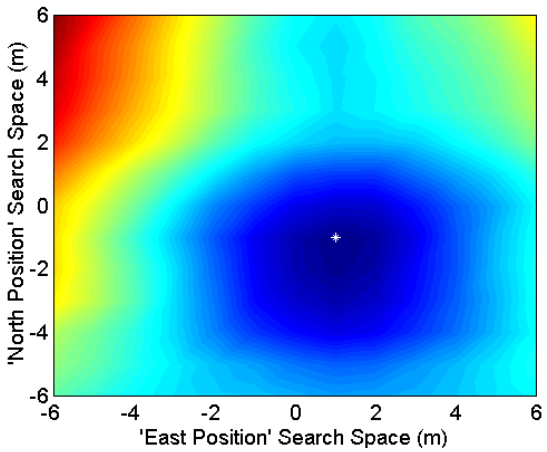

Figure 7, Position Search at GPS Time = 315280.2883 '∗' Marks Minimum Sum of Squares

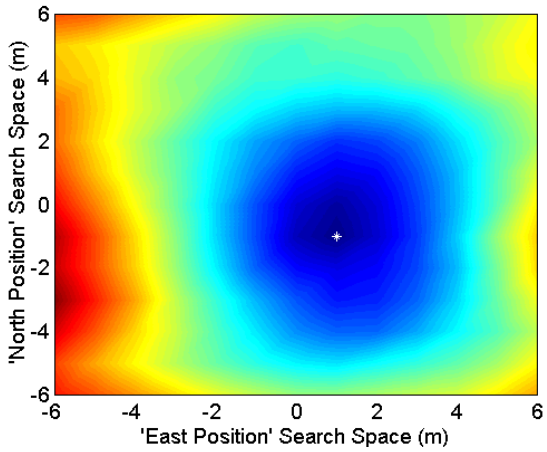

Figure 8, Position Search at GPS Time = 315280.4882
'' Marks Minimum Sum of Squares*

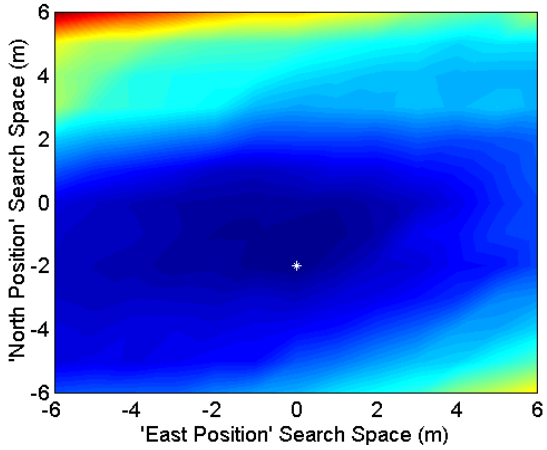

Figure 9, Position Search at GPS Time = 315280.6882
'' Marks Minimum Sum of Squares*

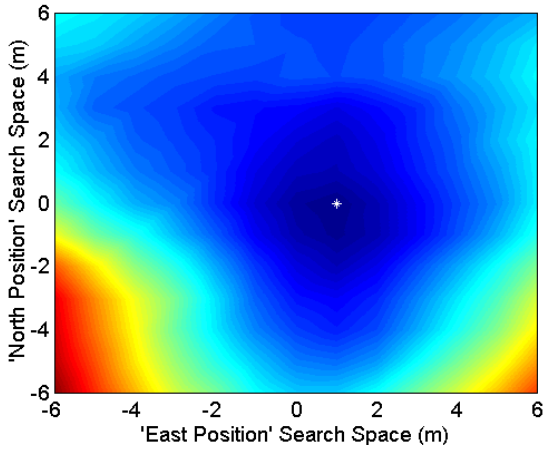

Figure 10, Position Search at GPS Time = 315280.8882
'' Marks Minimum Sum of Squares*

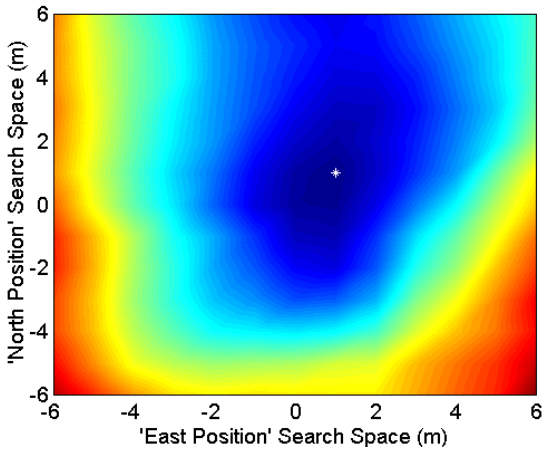

Figure 11, Position Search at GPS Time = 315281.0882
'' Marks Minimum Sum of Squares*

Figures 12, 13, 14, and 15 show the measurement solutions for altitude, roll, pitch and heading. The graphs differ from the previous graphs in that they represent one-dimensional quantities with time on the y-axis, the estimate on the x-axis, and the color representing the SS. The white line in the picture connects the minimum SS at each time epoch. The RMS value of the altitude is 1.3 m, the RMS value of the roll is 0.2 deg, the RMS value of the pitch is 0.8 deg, and the RMS value of the heading is 0.4 deg. The data used in these plots were collected at an altitude of 450 m AGL. After the 10 times down-sampling of the data, the calculated across-track measurement spacing was about 1 m. As the altitude AGL is increased the LiDAR coverage area increases which can significantly improve accuracies.

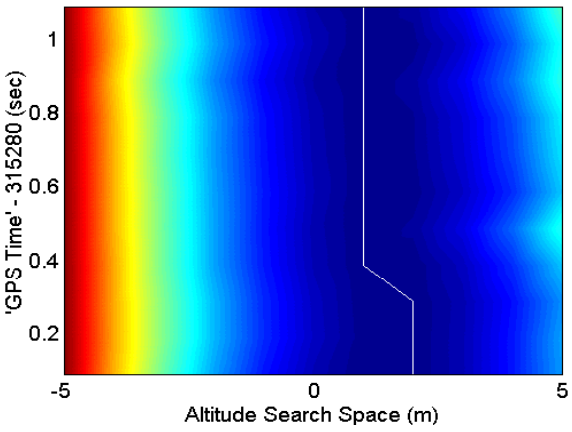

Figure 12, Altitude Search
GPS Time = 315280.0883 - 315281.0882
White = Minimum Sum of Squares

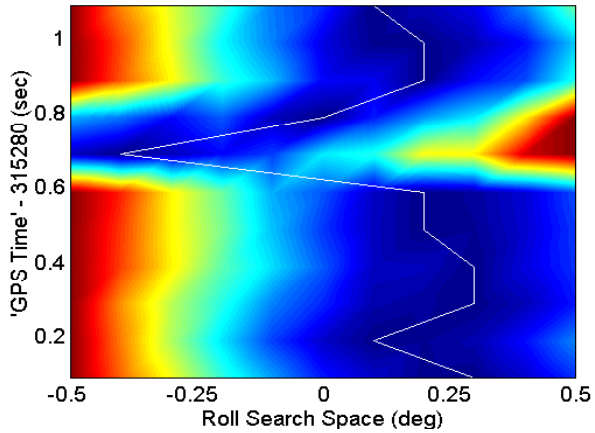

Figure 13, Roll Search
GPS Time = 315280.0883 - 315281.0882
White = Minimum Sum of Squares

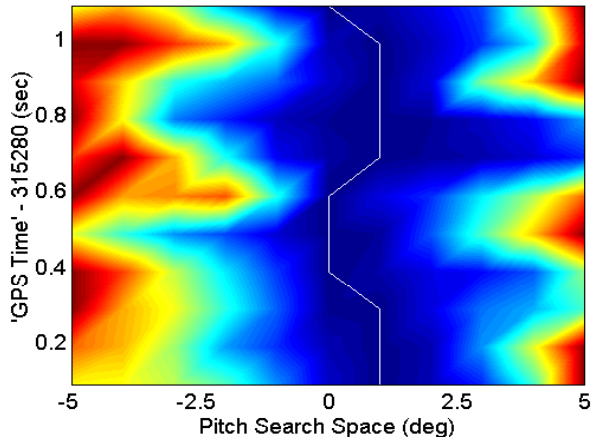

Figure 14, Pitch Search
GPS Time = 315280.0883 - 315281.0882
White = Minimum Sum of Squares

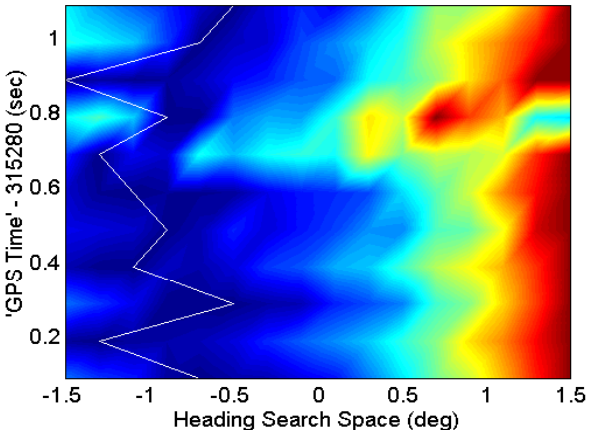

Figure 15, Heading Search
GPS Time = 315280.0883 - 315281.0882
White = Minimum Sum of Squares

8. SUMMARY, CONCLUSIONS, FUTURE PLANS

This paper provides a concept exploration of LiDAR based terrain navigation. Some of the current obstacles limiting the implementation of an all-weather LiDAR based terrain navigation system are discussed as well as possible ways to overcome these obstacles. A method to perform terrain navigation using the LiDAR is introduced, and samples of measurement solutions are presented.

Results show horizontal radial position estimates computed over one second of data have an RMS error value of 1.7 m. Results also show altitude estimation with an error RMS value of 1.3 m, roll estimation with an RMS error value of 0.2 degs, pitch estimation with and RMS error value of 0.8 degs, and heading estimation with an RMS error value of 0.4 degs.

Future work will be concentrated on the implementation of the LiDAR-based terrain navigation system. This analysis will include all required navigation parameters such as accuracy and integrity. Research is also under way to find worst-case weather scenarios and estimate laser power needed to operate in these conditions. Future plans also include the investigation into other areas of LiDAR use such as: high-accuracy attitude and heading information, in-flight IMU error calibration, aircraft surface movement guidance, runway incursion detection, and the integration with Synthetic Vision Systems (SVS).

ACKNOWLEDGMENTS

This paper would not have been possible without the help of many individuals. We would like to thank the US Army Joint Precision Strike Demonstration (JPSD) project office for use of their LiDAR equipment. Thanks go to the support staff from Optech, namely Bill Gutelius, Warrick Hadley, and Lindsay MacDonald, for their expertise on the LiDAR installation and help in the LiDAR data processing. Finally we must thank the NASA DC-8 flying laboratory crew and support staff for their flexibility and help collecting the data.

REFERENCES

[1] Kayton, M., W. R. Fried, Avionics Navigation Systems, Second Edition, John Wiley & Sons, Inc., New York, 1997.

[2] Wehr, A., U. Lohr, "Airborne laser scanning – an introduction and overview," ISPRS Journal of Photogrammetry & Remote Sensing 54, pp. 68-82, 1999.

[3] Huising, E.J., L. M. Gomes Pereira, "Errors and accuracy estimates of laser data acquired by various laser scanning systems for topographic applications," ISPRS Journal of Photogrammetry & Remote Sensing 53, pp. 245-261, 1998.

[4] Baltsavias, E. P., "Airborne laser scanning: basic relations and formulas," ISPRS Journal of Photogrammetry & Remote Sensing 54, pp 199-214, 1999.

[5] Hostetler, L. D., R. D. Andreas, "Nonlinear Kalman filtering techniques for terrain-aided navigation," *IEEE Transactions on Automatic Control*, AC-28, pp. 315–323, March 1983.

[6] Klass, P. J. , "New guidance system being tested," Aviation Week and Space Technologies, pp. 48-51, Feb. 25, 1974.

[7] Baird, C. A., M. R. Abramson, "A comparison of several digital map-aided navigation techniques," Proceedings of the IEEE PLANS, pp. 286-293, 1984.

[8] Hostetler, L. D., R. D. Andreas, R. C. Beckman, "Continuous Kalman updating of an inertial navigation system using terrain measurements," *IEEE NAECON*, CH1336, 1978.

[9] Baird, C. A., "Map-aided navigation system employing TERCOM-SITAN signal processing," United States Patent 4,829,304, May 9 1989.

[10] McGuffin, J. T., "Terrain referenced navigation adaptive filter distribution," United States Patent 5,331,562, July 19, 1994.

[11] Runnalls, A. R., "A Bayesian Approach To Terrain Contour Navigation,"AGARD Unclassified paper No. 43, Guidance and Control Panel, 40th Symposium, May 1985.

[12] Chan, L. C., F. B. Snyder, "System for correlation and recognition of terrain elevation," United States Patent 4,584,646, April 22, 1986.

[13] Evans G. W, J. E. Paul, "Autonomous Check Pointing Navigational System for an Airborne Vehicle," United States Patent 4,179,693, December 18, 1979.

[14] Webber W. F., "Vehicle Guidance System," United States Patent 4,144,571, March 13, 1979.

[15] Sliney, D., M. Wolbarsht, Safety with Laser and Other Optical Sources, Plenum Press, New York, 1980.

[16] American National Standards Institute, "Safe Use of Lasers," ANSI Standard Z136.1 – 2000, Laser Institute of America, Orlando, Florida, 2000.

[17] Burnham, R. L., J. J. Kasinski, L. R. Marshall, "Eye-safe laser system," US Patent No. 5,181,211, Jan 19, 1993.

[18] Webb, M. S., P. F. Moulton, J. J. Kasinski, R. L. Burnham, G. Loiacono, R. Stolzenberger, "High-Average-Power KTA OPO," www.qpeak.com/Papers/Hapopo.htm, August 22, 2003.